NASA/TM—2017-219490

Mapping Bone Mineral Density Obtained by Quantitative Computed Tomography to Bone Volume Fraction

James A. Pennline
Glenn Research Center, Cleveland, Ohio

Lealem Mulugeta
Universities Space Research Association, Houston, Texas

June 2017

NASA STI Program . . . in Profile

Since its founding, NASA has been dedicated to the advancement of aeronautics and space science. The NASA Scientific and Technical Information (STI) Program plays a key part in helping NASA maintain this important role.

The NASA STI Program operates under the auspices of the Agency Chief Information Officer. It collects, organizes, provides for archiving, and disseminates NASA's STI. The NASA STI Program provides access to the NASA Technical Report Server—Registered (NTRS Reg) and NASA Technical Report Server—Public (NTRS) thus providing one of the largest collections of aeronautical and space science STI in the world. Results are published in both non-NASA channels and by NASA in the NASA STI Report Series, which includes the following report types:

- TECHNICAL PUBLICATION. Reports of completed research or a major significant phase of research that present the results of NASA programs and include extensive data or theoretical analysis. Includes compilations of significant scientific and technical data and information deemed to be of continuing reference value. NASA counter-part of peer-reviewed formal professional papers, but has less stringent limitations on manuscript length and extent of graphic presentations.

- TECHNICAL MEMORANDUM. Scientific and technical findings that are preliminary or of specialized interest, e.g., "quick-release" reports, working papers, and bibliographies that contain minimal annotation. Does not contain extensive analysis.

- CONTRACTOR REPORT. Scientific and technical findings by NASA-sponsored contractors and grantees.

- CONFERENCE PUBLICATION. Collected papers from scientific and technical conferences, symposia, seminars, or other meetings sponsored or co-sponsored by NASA.

- SPECIAL PUBLICATION. Scientific, technical, or historical information from NASA programs, projects, and missions, often concerned with subjects having substantial public interest.

- TECHNICAL TRANSLATION. English-language translations of foreign scientific and technical material pertinent to NASA's mission.

For more information about the NASA STI program, see the following:

- Access the NASA STI program home page at http://www.sti.nasa.gov

- E-mail your question to help@sti.nasa.gov

- Fax your question to the NASA STI Information Desk at 757-864-6500

- Telephone the NASA STI Information Desk at 757-864-9658

- Write to:
  NASA STI Program
  Mail Stop 148
  NASA Langley Research Center
  Hampton, VA 23681-2199

NASA/TM—2017-219490

Mapping Bone Mineral Density Obtained by Quantitative Computed Tomography to Bone Volume Fraction

James A. Pennline
Glenn Research Center, Cleveland, Ohio

Lealem Mulugeta
Universities Space Research Association, Houston, Texas

National Aeronautics and
Space Administration

Glenn Research Center
Cleveland, Ohio 44135

June 2017

Level of Review: This material has been technically reviewed by technical management.

Available from

NASA STI Program
Mail Stop 148
NASA Langley Research Center
Hampton, VA 23681-2199

National Technical Information Service
5285 Port Royal Road
Springfield, VA 22161
703-605-6000

This report is available in electronic form at http://www.sti.nasa.gov/ and http://ntrs.nasa.gov/

Mapping Bone Mineral Density Obtained by Quantitative Computed Tomography to Bone Volume Fraction

James A. Pennline
National Aeronautics and Space Administration
Glenn Research Center
Cleveland, Ohio 44135

Lealem Mulugeta
Universities Space Research Association
Houston, Texas 77058

Summary

Methods for relating or mapping estimates of volumetric bone mineral density (vBMD) obtained via quantitative computed tomography (QCT) to bone volume fraction (BVF) are outlined mathematically. The methods are based on definitions of bone properties, cited experimental studies, and regression relations derived from those studies for trabecular bone in the proximal femur. BVF values calculated from four different methods were compared with the experimental average and numerical range of values obtained from the intertrochanteric region of male and female human subjects, aged 18 to 49. The BVF values computed from the conversion methods used data from two sources. One source provided pre-bed-rest vBMD values in the intertrochanteric region from 24 bed rest subjects who participated in a 70-day study. Another source provided preflight vBMD values from 18 astronauts who spent 4 to 6 months on the International Space Station (ISS). To aid the use of a mapping from BMD to BVF, the discussion includes how to formulate the conversions for the purpose of computational modeling. An application of the conversions would be used to aid in computational modeling of time-varying changes in vBMD as they relate to changes in BVF via bone remodeling and/or modeling.

Introduction

Most computational models of bone remodeling or bone adaptation track changes in apparent density (Refs. 1 to 3) or bone volume fraction (BVF) (Refs. 4 to 6), but in vivo measurements of bone density are given in terms of bone mineral density (BMD). Areal BMD (aBMD) is defined as bone mineral content divided by total area, g/cm^2. Volumetric BMD (vBMD) is bone mineral content divided by total volume, g/cm^3. Dual-energy x-ray absorptiometry, an enhanced form of x-ray technology, is an established standard bone density scanning method for measuring aBMD (Ref. 7). One medical technique that measures vBMD is quantitative computed tomography (QCT) (Ref. 8). QCT uses a standard x-ray computed tomography (CT) scanner with a calibration standard to convert Hounsfield units of the image to vBMD values. In order to compare model prediction to experimental data, a method of converting aBMD or vBMD to BVF is needed.

In NASA's Digital Astronaut Project (DAP), the musculoskeletal research component has as a current task the development of a computational bone physiology model for space flight bone physiology analysis (Ref. 9). One aim is to understand the changes in vBMD, particularly bone loss, at various bone sites and the response to in-flight and postflight exercise countermeasures. The mathematical formulation describes the removal and replacement of bone via bone remodeling and simulates changes in bone in terms of changes in BVF. The changes are observed in subjects of bed rest studies that simulate microgravity and in astronauts during and after 4- to 6-month periods on the International Space Station (ISS). In addition, the DAP bone physiology model can add higher fidelity by breaking up BVF into mineralized volume fraction, M, and osteoid volume fraction, O:

$$BVF = M + O \tag{1}$$

Because of its three-dimensional capability and its ability to provide specific data for the separate cortical and trabecular regions of bone, the DAP bone physiology model is developed directly for QCT data. Human QCT scans are generally lower resolution to minimize radiation health risks, which in turn tends to prevent the determination of BVF via image processing software. Therefore, a method for converting initial vBMD data to initial BVF is needed in order to simulate time-course changes in BVF that can then be converted back to vBMD. This study presents a number of conversion methods with a focus on the trabecular region of the proximal femur. Terms used in this paper are defined in the Appendix.

Acronyms

aBMD	areal bone mineral density
BMD	bone mineral density
BVF	bone volume fraction
CFT	countermeasures and functional testing
CT	computed tomography
DAP	Digital Astronaut Project
ISS	International Space Station
mCT	microcomputed tomography
QCT	quantitative computed tomography
vBMD	volumetric bone mineral density

Symbols

aBMD	areal bone mineral density
BMD	bone mineral density
BVF	bone volume fraction
M	mineralized volume fraction
O	osteoid volume fraction
vBMD	volumetric bone mineral density
α	ash fraction $\alpha = \frac{\rho_{ash}}{\rho_{app}}$
ρ	density

Relations and Formulas

Algorithms for the conversions are based in part on using linear correlation relations obtained from experimental studies that relate QCT-derived vBMD, ρ_{QCT}, to ash density, ρ_{ash}, and ash density to

apparent dry density, ρ_{app}. From experimental results on proximal femur samples, conversion from ρ_{QCT} to ρ_{ash} for combined cortical and trabecular developed by Keyak et al. (Refs. 10 to 11) is given by

$$\rho_{ash} = 0.887\rho_{QCT} + 0.0633 \tag{2}$$

The experiments did not include results of correlating ρ_{app} to ρ_{ash} prior to ashing for the proximal femur. However, an earlier work by Keyak et al. (Ref. 12) involving the proximal tibia trabecular region produced the relation

$$\rho_{app} = 1.66\rho_{ash} + 0.00457 \tag{3}$$

Similar experimental work by Schileo et al. (Ref. 13) using human femur specimens obtained the following regressions for trabecular specimens (4a), which was not significantly different from the regression line for cortical specimens (4b):

$$\rho_{app} = 1.64\rho_{ash} + 0.01 \tag{4a}$$

$$\rho_{app} = 1.58\rho_{ash} + 0.11 \tag{4b}$$

In addition to the experimentally derived regressions shown above, key experimental studies have been used to obtain relational estimates of true density and BVF. Experimental work from Keller (Ref. 14) computed ρ_{ash}, ρ_{app}, and ash fraction α from 199 spine specimens and 297 femur specimens. Ash fraction values ranged from 0.174 to 0.662 with a mean spine value of 0.610 and a mean femur value of 0.583. Hernandez et al. (Ref. 15) concluded from that study that the ash fraction of unmineralized osteoid, $\alpha = 0$, and fully mineralized bone, $\alpha = 0.7$, covered most of the range of values observed in human bone. Using dry tissue densities of 1.41 g/cm^3 for unmineralized osteoid and 2.31 g/cm^3 for mineralized bone (Refs. 16 to 18), a linear approximation for true density through the points (0, 1.41 g/cm^3) and (0.7, 2.31 g/cm^3) was obtained:

$$\rho_t \cong 1.41 + 1.29\alpha \tag{5}$$

This allowed BVF to be approximated as

$$BVF \approx \frac{\rho_{app}}{\rho_t} \tag{6}$$

Another way to obtain BVF is to piece together the two volume fractions. *M* can be obtained from the following definition. For a given segment or volume of bone, the ash density equals *M* times the true dry density times the maximum ash fraction.

$$\rho_{ash} = M \cdot 2.31 \cdot (\alpha_{max}) \tag{7a}$$

$$M = \frac{\rho_{ash}}{2.31 \cdot (\alpha_{max})} \tag{7b}$$

Then from the ratio $\alpha = \rho_{ash} / \rho_{app}$, *O* can be solved for from the equation

$$\alpha = \frac{M \cdot 2.31 \cdot (\alpha_{max})}{M \cdot 2.31 + O \cdot 1.41} \tag{8}$$

It is important to note that the value of α_{max} is assumed to be near 0.7, according to the work of Hernandez et al. (Ref. 15), as most of that work, such as Equation (5), is based on the work of Keller (Ref. 14). The work of Schileo et al. (Ref. 13), however, revealed the ρ_{ash} / ρ_{app} ratio to be fairly constant at a value of 0.6 in human femoral cortical bone. Additionally, their initial analysis showed that the average ratio for trabecular bone was lower, 0.46, with a greater variation, 0.34 to 0.62. Consequently, Schileo et al. extended their experimental study to include a set of trabecular specimens from the same femur that were smaller than those from the initial analysis. For the new specimen set, the average ρ_{ash} / ρ_{app} ratio was found to be 0.6 with a range of 0.54 to 0.63 and did not differ statistically from that of the cortical specimens. Schileo et al. attributed the difference in ratio between the set of smaller specimens and the set of initial larger specimens with higher density trabecular bone to possible experimental error in the measurement of ρ_{app}. There could be an overestimation of ρ_{app} in those larger, high-density specimen cases, as it is more difficult in the experimental process to assure complete removal of water and marrow from the cavities. However, it appeared that the ratio could be accurately measured in low-density trabecular specimens, independent of size. In fact, a 0.6 ratio was found for some low-density large trabecular specimens. Based on these findings, Schileo et al. rejected their initial hypothesis that the ratio decreases as tissue density increases, and α was assumed equal to 0.6 for the whole density range.[1]

Conversion Methods

Outlines of the methods are given in terms of initialization of a computational model's bone volume fraction, BVF_0 value from an initial $vBMD_0$ value. Simulated changes in *BVF* can then be mapped back to *vBMD*. The first three steps (a, b, and c) are the same for each of the conversion methods.

Given a *vBMD* value in terms of ρ_{QCT} as measured by QCT,

a. Convert ρ_{QCT} to ρ_{ash} by Equation (2).

b. Compute ρ_{app} by Equation (4).[2]

c. Calculate initial ash fraction $\alpha = \frac{\rho_{ash}}{\rho_{app}}$.

[1]A suggestion was made that this could explain the results reported by Hernandez et al. from the large dataset of Keller where a low ratio was reported for high-density trabecular bone.

[2]There is little difference between Equations (2) and (4). Equation (4) was derived using data from femur specimens, which is the site of interest, whereas Equation (2) was derived using data from tibia specimens.

Method 1: Uses only the single volume fraction.

d. Estimate true tissue density ρ_t by Equation (5).

e. BVF is then given by

$$BVF_1 = \frac{\rho_{app}}{\rho_t} \tag{9}$$

In computational simulations, time-varying changes in BVF_1 can be converted back to time-varying changes in *vBMD* via changes in ash fraction, apparent density, and ash density. From Equation (9), substitute ρ_{ash}/ρ_{app} for ash fraction α in the definition of ρ_t and rearrange to obtain

$$BVF_1(t) \cdot (1.41 \cdot \rho_{app}(t) + 1.29 \cdot \rho_{ash}(t)) = (\rho_{app}(t))^2 \tag{10}$$

Next, substitute for ρ_{ash} in terms of ρ_{app} from Equation (4) and solve the resulting quadratic for $\rho_{app}(t)$. Time-varying changes in ash density $\rho_{ash}(t)$ can then be obtained via Equation (4), followed by time-varying changes in *vBMD*(*t*) via Equation (2).

The following methods split *BVF* into *M* plus *O*.

Method 2: Uses estimate of true density formula, Equations (5) and (6).

d. Obtain initial volume fraction M_0 from Equation (7b) using $\alpha_{max} = 0.7$.

e. Estimate initial true tissue density ρ_t by Equation (5) using initial α_0.

f. Solve for initial osteoid volume fraction O_0 from Equation (6):

$$\frac{\rho_{app}}{BVF_2} = \frac{M_0 \cdot (2.31) + O_0 \cdot (1.41)}{M_0 + O_0} = \rho_t \tag{11a}$$

$$O_0 = \left(\frac{2.31 - \rho_t}{\rho_t - 1.41} \right) \cdot M_0 \tag{11b}$$

g. BVF is given by

$$BVF_2 = M_0 + O_0. \tag{12}$$

Time-varying changes $BVT_2(t) = M(t) + O(t)$ can again be converted back to time-varying changes in *vBMD* from computational simulations of *M*(*t*) and *O*(*t*). From Equation (7a), obtain time-varying changes in $\rho_{ash}(t)$ and then *vBMD*(*t*) via Equation (2).

Method 3: Uses definition of ash fraction, Equation (8) with $\alpha_{max} = 0.7$.

d. Obtain initial volume fraction, M_0, from Equation (7b).

e. Solve for O_0 from Equation (8) using α from step c.

$$O_0 = \frac{M_0 \cdot (2.31) \cdot (\alpha_{max} - \alpha_0)}{(1.41) \cdot \alpha_0} \tag{13}$$

f. BVF is given by

$$BVF_3 = M_0 + O_0 \tag{14}$$

In this case, M_0 and O_0 are provided by the steps under Method 3. Time-varying changes in $M(t)$ and $O(t)$ can be used to track $\alpha(t)$ via Equation (8). Then, time-varying changes in *vBMD* can be recovered by first obtaining $\rho_{ash}(t)$ from Equation (7a) and then *vBMD*(t) via Equation (2).

Method 4: Uses definition of ash fraction, Equation (8) with $\alpha_{max} = 1.0/1.64$. This value of α_{max} is obtained from the maximum value of the ratio

$$\alpha = \frac{\rho_{ash}}{1.64\rho_{ash} + 0.01} \tag{15}$$

as a function of ρ_{ash}. The steps in Method 4 are the same as those in Method 3, resulting in

$$BVF_4 = M_0 + O_0 \tag{16}$$

In this case, O_0 is calculated from Equation (13) with the smaller value of α_{max}.

Validation of Bone Volume Fractions Obtained by Conversion

To test if *BVF* values calculated by the conversion methods are within appropriate ranges that can be expected for healthy adults, the literature was searched for articles that reported *BVF* values for the proximal femur. A study by Tsangari et al. (Ref. 19) reported trabecular *BVF* values for the intertrochanteric region of the proximal femur for male and female adults aged 18 to 49. These results are summarized in Table I.

Two sets of trochanteric *vBMD* data were subjected to conversion via each method, as summarized in Table II. One set represents preflight *vBMD* data of the trochanteric region in 18 astronauts making ISS flights of 4 to 6 months (Ref. 20). The other set represents the pre-bed-rest *vBMD* of the trochanter region in 24 exercisers of a 70-day bed rest study, Countermeasures and Functional Testing in Bed Rest (CFT 70). QCT *vBMD* data was provided by the NASA Johnson Space Center Bone Lab through the NASA Life Sciences Data Archive.

Comparing the calculated *BVF* values to the experimental values presented in Table I, Methods 2 and 4 present an average and standard deviation for the CFT 70 bed rest group that is inside and toward the lower half of the range for both the male and female experimental averages and standard deviations. For the astronaut group, calculated *BVF* values for Methods 2 and 4 are close to the female experimental values in terms of average and standard deviation and are fairly centered inside the experimental range of values for males. The calculated values of Methods 1 and 3 for the astronaut group lay inside of the male experimental range in terms of average and standard deviation and are shifted toward the higher half.

TABLE I.—EXPERIMENTAL VALUES FOR TRABECULAR BONE VOLUME FRACTION (BVF) FOR PROXIMAL FEMUR REPORTED IN REFERENCE 19

Gender	Age range	Trabecular BVF
Female n = 13	18 to 49	0.146±0.04
Male n = 14	18 to 49	0.151±0.064

TABLE II.—PREDICTED TRABECULAR BONE VOLUME FRACTION (BVF) VALUES FOR EACH METHOD

Trabecular vBMD data source	Age range	Calculated BVF values			
		Method 1	Method 2	Method 3	Method 4
CFT[a] 70 bed rest study n = 24	24 to 42 32±5.3	0.145±0.02	0.136±0.02	0.149±0.02	0.139±0.02
Lang et al. (Ref. 20) n = 18	44.6±4.0	0.151±0.017	0.142±0.016	0.156±0.017	0.145±0.016

[a]Countermeasures and functional testing

Since the standard deviations of the calculated *BVF* values for each method are small, a clearer comparison between the calculated *BVF* values of the methods and the experimental *BVF* values can be made by observing the distribution of the individual *BVF* values of the methods. These are illustrated in Figure 1 for the CFT 70 bed rest subjects and in Figure 2 for the astronauts.

This makes a much clearer evaluation of the methods. As shown in Figures 1 and 2, the distribution of the individual *BVF* values falls within the male experimental range for all four methods. For the bed rest subjects, distributions of Methods 2 and 4 are shifted toward the lower end of the experimental ranges, with several values outside the lower end of the female experimental range, which explains the lower averages in Table II. However, as the bed rest subjects are all males, their *BVF* values are all within the experimental range for the four methods.

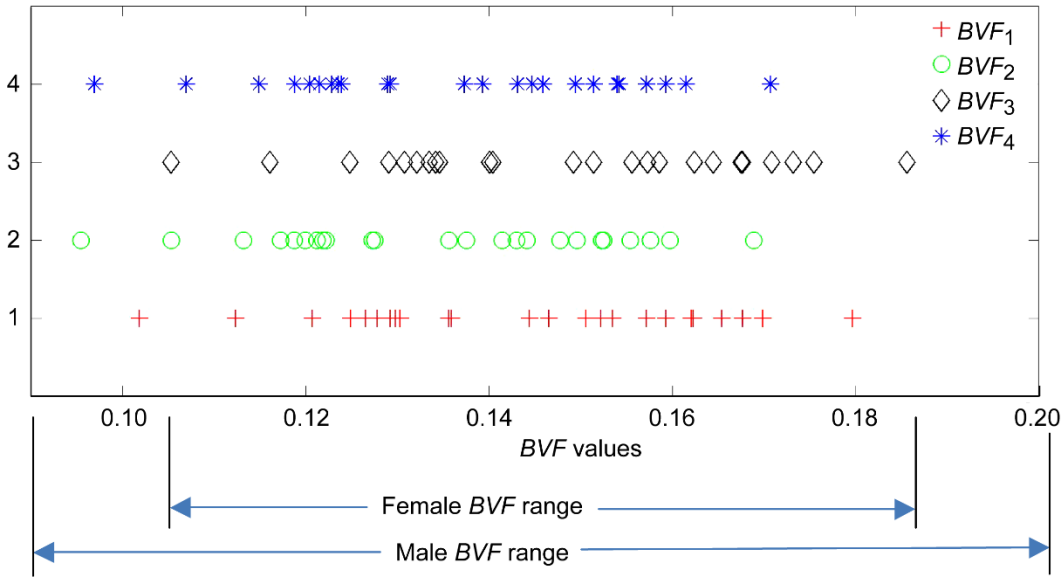

Figure 1.—Distribution of bone volume fraction (*BVF*) values of individual bed rest subjects for Methods 1 to 4. The range of experimental values for females and males according to the average and standard deviation are shown below the horizontal scale of *BVF* values.

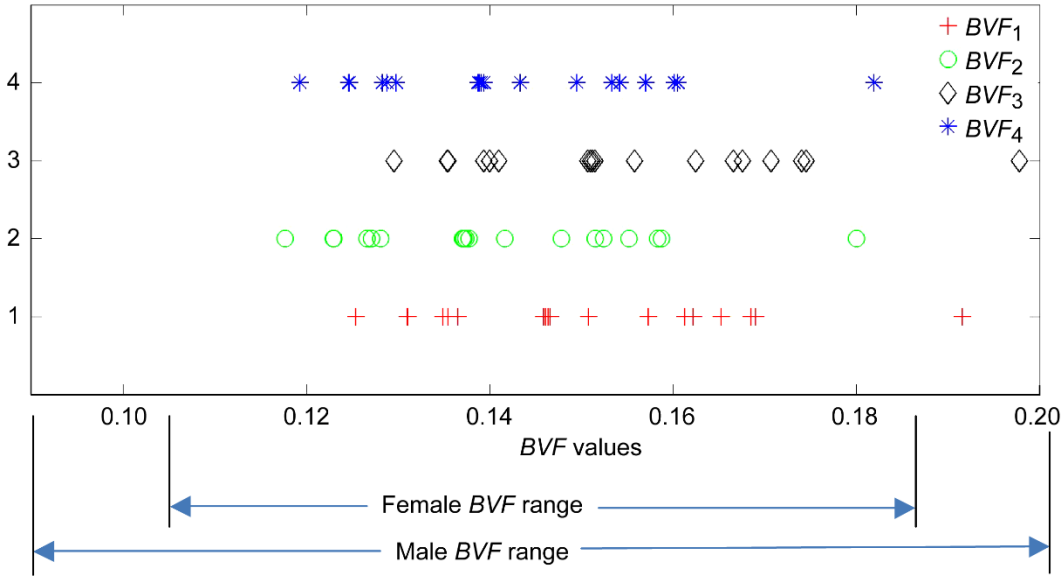

Figure 2.—Distribution of bone volume fraction (*BVF*) values of individual astronauts for Methods 1 to 4. The range of experimental values for females and males according to the average and standard deviation are shown below the horizontal scale of *BVF* values.

TABLE III.—MINERALIZED AND OSTEOID VOLUME FRACTIONS FOR AVERAGE ASTRONAUT *vBMD* = 0.148 g/cm^3

Method 2		Method 3		Method 4 $\alpha_{max} = 1/1.66$		Method 4 $\alpha_{max} = 0.60103$	
M	*O*	*M*	*O*	*M*	*O*	*M*	*O*
0.1203	0.0217	0.1203	0.0363	0.1381	0.0071	0.1401	0.0038

Compared with the distribution of *BVF* values of the bed rest subjects, the distribution of the *BVF* values of the astronauts is shifted toward the higher end of the experimental ranges for each method. This is reasonable, as the astronauts are a healthier group that undergoes strength conditioning and training prior to flight.

The same article that reports intertrochanteric *BVF* values (Ref. 19) also has mean *O* values. Compared with *M*, this normally tends to be small. The reported values are on the order of 10^{-4} for females between 18 and 49 and 10^{-3} for males between 18 and 49. Table III shows the values of Methods 2 to 4 for the average astronaut *vBMD* of 0.148 g/cm^3.

For the last set, the value of 0.60103 is obtained from Equation (15) by setting the value of ρ_{ash} to 1.2, which was usually the estimated top value of ρ_{ash} in Reference 12.

For consistency, modeling that uses the sum of mineralized and osteoid volume fractions should be the same or close to the values of the single volume fraction. To achieve that, Methods 2 and 4 can be adjusted.

For Method 2, consider the following alternative:

Method 2a:

d. Obtain initial volume fraction, M_0, from Equation (7b).
e. Set $M_0+O_0 = BVF_1$ defined in Equation (9).
f. Solve for O_0.

$$O_0 = \frac{\rho_{app}}{\rho_t} - M_0 \tag{17}$$

g.
$$BVF_2a = M_0 + O_0 \tag{18}$$

BVF_2a will then have the same values as BVF_1.

For Method 4, the results of the study by Schileo et al. (Ref. 13) for smaller trabecular specimens can be considered. In those cases, some variation in ash fraction up to 0.63 was observed. This suggests using an estimate of α_{max} of about 0.63 to 0.65. So the following alternative for Method 4 is defined:

Method 4a:

d. Obtain initial volume fraction, M_0, from Equation (7b) with $\alpha_{max} = 0.65$.

$$M = \frac{\rho_{ash}}{2.31 \cdot (0.65)} \tag{19}$$

e. Solve for O_0 from Equation (8).

$$O_0 = \frac{M_0 \cdot (2.31) \cdot (0.65 - \alpha_0)}{(1.41) \cdot \alpha_0} \tag{20}$$

f.
$$BVF_4a = M_0 + O_0 \tag{21}$$

For Method 4a, $BVF_4a = 0.144 \pm 0.02$ for the bed rest subjects, which is similar to BVF_1 in Figure 1. For the astronauts, $BVF_4a = 0.150 \pm 0.019$, which is similar to BVF_1 in Figure 2.

Alternately, Method 1 can be adjusted. Since the work of Keyak et al. and Schelio et al. suggests a relatively constant ash fraction value of 0.6, let 1/1.64 = 0.6097 be an estimate of the maximum value of α_{max} from Equation (15) and replace Equation (5) with a line through (0, 1.41g/cm^3) and (0.6097, 2.31g/cm^3). This will result in an equation that will give a larger value of true density ρ_t in Equation (9) and hence a smaller value of BVF_1. This will generate values of BVF_1 close to the values of Method 4.

Bone Volume Fraction From Microcomputed Tomography

A study by Tassani et al. (Ref. 21) to investigate whether tissue mineral density can be assumed a constant in adult human bone used microcomputed tomography (mCT) analysis. Ninety-six specimens from various lower limb sites (tibias and femurs) were extracted from two female cadavers. BVF was measured via mCT, and specimens were ashed to gravimetrically measure ρ_{ash}. Performance of a regression analysis between ρ_{ash} and BVF for the pooled groups of trabecular and cortical specimens obtained the following relation:

$$\rho_{ash} = 1.18\,BVF_{mct} + 0.01 \tag{22a}$$

An intrasite analysis was performed on a second group of 19 trabecular specimens extracted from femoral heads of different donors. Performance of a regression analysis of ρ_{ash} over BVF gave the relation

$$\rho_{ash} = 0.99\,BVF_{mct} + 0.04 \tag{22b}$$

If the data were to be used to obtain *BVF* values directly from ρ_{ash}, one might solve for BVF_{mct} in either equation to get a valid estimate. However, forming a regression of *BVF* on ρ_{ash} would not generally give the same equation. Unfortunately, the data was not available to perform the regression analysis that way. If Equation (22a) is reversed, values of ρ_{ash} from Equation (2) generate values of BVF_{mct} = 0.156±0.019 for the astronaut's *vBMD* and BVF_{mct} = 0.149±0.02 for the bed rest subject's *vBMD*. Values generated from the reverse of Equation (22b) and the reverse of the regression from the trabecular group of the original 96 specimens produced very similar results. These are average values similar to those values listed under Method 3 in Table II. It would be worthwhile to obtain the data from the study by Tassani et al. and perform a regression of *BVF* on ρ_{ash} to obtain the correct reverse of Equations (22a) or (22b), then substitute the values of ρ_{ash} from Equation (2) into the reverse of Equation (22a) or (22b) and compare the results to the other methods. This would be the simplest and most direct method of conversion.

DAP Computational Bone Physiology Method

Currently the DAP model that predicts changes in *BVF* uses conversion Method 2 for converting *vBMD* into *BVF* by combining *M* and *O*. This early version of the conversion is based on knowledge available at the time of the work of Keyak et al. (Ref. 12) and Hernandez et al. (Ref. 15). This method was used in the validation analysis of the femoral neck model. At that time, the intention was to use a modulus formula developed by Hernandez et al. in the finite element model for bone that is coupled with the model's bone physiology component. In the process of validating the model for the femoral neck, the modulus formula was changed to a formula by Keyak et al. (Ref. 11). Further literature research yielded additional knowledge of the other cited work. This, along with continuing mathematical research into other conversion possibilities, and prompted by a desire to extend the model to the full proximal femur, led to consideration of the other methods. As a result, researchers plan to modify the code to use Method

4 for consistency, as it makes use of the Keyak and Schileo ash fraction values of about 0.6. Method 4 appears to validate *O* values better, as indicated by Table III. Also planned is completion of an updated, shorter simulation in which BVF changes are not split into *M* and *O*.

Conclusions

The methods outlined here for converting bone mineral density (BMD) derived via quantitative computed tomography (QCT) to an approximated bone volume fraction (BVF) in trabecular bone of the proximal femur are based on multiple experimental studies, correlation relations derived from those studies, and definitions of bone properties. The best way to validate the methods would be to apply the conversion methods to the BMD values of the subjects used to obtain the experimental ranges of BVF values, but that data is unavailable. Although the BVF values predicted by the methods differ, they all fall within a range of experimental values for the intertrochanteric region. Judgment of the methods was thus limited to how well the distribution of BVF values obtained from pre-bed-rest BMD of 24 subjects and preflight BMD of 18 astronauts covers the experimental range. The need for Digital Astronaut Project model changes in BVF derived by Method 1 to be consistent with changes in BVF derived by methods that combine *M* and *O*, such as Methods 2, 3, and 4, was also considered. Ultimately, with any method, the interest will be in validation of the computational model. That involves an analysis of how well the computational model's resulting changes in vBMD compare with experimental changes in vBMD.

Appendix—Definitions

- Apparent density—Weight of bone tissue divided by total volume of segment or specimen
- Real density—Weight of bone tissue divided by total volume of bone tissue (real volume)
  - Can be referred to as true density
  - Compact bone approximately constant—1.9 kg/cm^3 (Ref. 22)
- Volumetric bone mineral density (vBMD)—Bone mineral content divided by total volume of bone segment. Measure of bone density reflecting strength of bones as represented by calcium content
- Ash density (apparent)—Ratio between ash weight and volume of sample of bone segment or specimen
- Bone volume fraction (BVF)—Volume of bone tissue divided by total volume of bone segment
  - Bone volume includes internal pores like lacunae and canaliculi.
  - Trabecular bone may have BVF ranging from just over 5 percent to a maximum of 60 percent.
- Ash fraction—Ashed mass of a bone sample divided by the dry mass of the same sample
  - Sometimes referred to as percent mineralization
  - Considered a standard for determining amount of mineralization
  - Has been used to estimate bone material properties such as elastic modulus (Ref. 14)
  - Calculation requires destructively ashing the specimen
  - The mathematical expression of the ratio can vary, although the expressions have the same meaning:

$$\text{ash fraction} = \text{ash mass/dry mass}$$

$$= \frac{\text{inorganic mass (mass of Ca hydroxyapatite)}}{\text{inorganic mass + organic mass}}$$

$$= \frac{\text{mineralized mass}}{\text{mineralized mass} + \text{unmineralized mass}}$$

References

1. Beaupré, G.S.; Orr, T.E.; and Carter, D.R.: An Approach for Time-Dependent Bone Modeling and Remodeling-Application: A Preliminary Remodeling Simulation. J. Orthop. Res., vol. 8, no. 5, 1990, pp. 662–670.
2. Hambli, R.: Connecting Mechanics and Bone Cell Activities in the Bone Remodeling Process: An Integrated Finite Element Modeling. Front. Bioeng. Biotechnol., vol. 2, 2014. http://www.pubmedcentral.nih.gov/articlerender.fcgi?artid=4126454&tool=pmcentrez&rendertype=abstract Accessed June 6, 2017.
3. Komarova, S.V., et al.: Mathematical Model Predicts a Critical Role for Osteoclast Autocrine Regulation in the Control of Bone Remodeling. Bone, vol. 33, no. 2, 2003, pp. 206–215.
4. Nyman, J.S., et al.: A Theoretical Analysis of Long-Term Bisphosphonate Effects on Trabecular Bone Volume and Microdamage. Bone, vol. 35, no. 1, 2004, pp. 296–305.
5. Pennline, James A.: Simulating Bone Loss in Microgravity Using Mathematical Formulations of Bone Remodeling. NASA/TM—2009-215824, 2009. http://ntrs.nasa.gov
6. Pivonka, P., et al.: Theoretical Investigation of the Role of the RANK-RANKL-OPG System in Bone Remodeling. J. Theor. Biol., vol. 262, no. 2, 2010, pp. 306–316.
7. El Maghraoui, A.; and Roux, C.: DXA Scanning in Clinical Practice. QJM, vol. 101, no. 8, 2008, pp. 605–617.
8. Adams, J.E.: Quantitative Computed Tomography. Eur. J. Radiol., vol. 71, no. 3, 2009, pp. 415–424.
9. Pennline, James A.; and Mulugeta, Lealem: A Computational Model for Simulating Spaceflight Induced Bone Remodeling. ICES2014–513–83, 2014.
10. Keyak, J.H., et al.: Predicting Proximal Femoral Strength Using Structural Engineering Models. Clin. Orthop. Relat. Res., vol. 437, 2005, pp. 219–228.
11. Keyak, J.H., et al.: Reduction in Proximal Femoral Strength Due To Long-Duration Spaceflight. Bone, vol. 44, no. 3, 2009, pp. 449–453.
12. Keyak, J.H.; Lee, I.Y.; and Skinner, H.B.: Correlations Between Orthogonal Mechanical Properties and Density of Trabecular Bone: Use of Different Densitometric Measures. J. Biomed. Mat. Res., vol. 28, no. 11, 1994, pp. 1329–1336.
13. Schileo, E., et al.: An Accurate Estimation of Bone Density Improves the Accuracy of Subject-Specific Finite Element Models. J. Biomech., vol. 41, no. 11, 2008, pp. 2483–2491.
14. Keller, T.S.: Predicting the Compressive Mechanical Behavior of Bone. J. Biomech., vol. 27, no. 9, 1994, pp. 1159–1168.
15. Hernandez, C.J., et al.: The Influence of Bone Volume Fraction and Ash Fraction on Bone Strength and Modulus. Bone, vol. 29, no. 1, 2001, pp. 74–78.
16. Martin, R.B.: Porosity and Specific Surface of Bone. Crit. Rev. Biomed. Eng., vol. 10, no. 3, 1984, 179–222.
17. Robinson, Robert A.: Physicochemical Structure of Bone. Clin. Orthop. Relat. Res., vol. 112, 1975, pp. 263–315. http://www.scopus.com/inward/record.url?eid=2-s2.0-0016560609&partnerID=tZOtx3y1 Accessed June 6, 2017.
18. Robinson, R.A.: Observations Regarding Compartments for Tracer Calcium in the Body. H.M. Frost, ed., Bone Biodyn., Little, Brown, Boston, 1963, pp. 423–439.
19. Tsangari, H.; Findlay, D.M.; and Fazzalari, N.L.: Structural and Remodeling Indices in the Cancellous Bone of the Proximal Femur Across Adulthood. Bone, vol. 40, no. 1, 2007, pp. 211–217. http://www.ncbi.nlm.nih.gov/pubmed/16934541 Accessed June 10, 2013.
20. Lang, T.F., et al.: Adaptation of the Proximal Femur to Skeletal Reloading After Long-Duration Spaceflight. J. Bone Miner. Res., vol. 21, no. 8, 2006, pp. 1224–1230. http://www.ncbi.nlm.nih.gov/pubmed/16869720 Accessed Feb. 18, 2014.
21. Tassani, S., et al.: Volume to Density Relation in Adult Human Bone Tissue. J. Biomech., vol. 44, no. 1, 2011, pp. 103–108.
22. The Physics Factbook: An Encyclopedia of Scientific Essays. http://hypertextbook.com/facts/2002/AnnaYarusskaya.shtml Accessed May 31, 2017.